Pergamon

0038-092X(96)00289-X

Solar Energy Vol. 56, No. 4, pp. 343–348, 1996

0038-092X/96 $15.00+0.00

POWER OUTPUT OF Al/SnO_2/*n*-Si SOLAR CELL

KESHAW SINGH and R. Y. TAMAKLOE
Department of Physics, University of Science and Technology, University Post Office, Kumasi, Ghana, West Africa

(Communicated by GERARD WRIXON)

Abstract—An Al/SnO_2/*n*-Si solar cell from *n*-type silicon (6.5 Ω-cm, ⟨100⟩) wafers using chemical vapour deposition (CVD) has been fabricated. The fabrication details, *I–V* characteristics determining conversion-efficiency (η_{max}), open circuit voltage (V_{oc}) and short circuit current (I_{sc}) have been presented. A maximum conversion efficiency of 6.3% for an unencapsulated cell of area 85.20 mm² has been obtained. Copyright © 1996 Elsevier Science Ltd.

1. INTRODUCTION

The basic phenomenon which takes place in solar cells is that the photons are absorbed in the semiconductor material and generate electron–hole pairs (Lim, 1983; Neville, 1978; Chalmers, 1976; Sze, 1981). Loferski (1976) found that the number of absorbed photons, having energy greater than the band gap, decreases as the band gap increases. He also studied the maximum solar energy conversion efficiency as a function of band gap. Silicon with a band gap of 1.1 eV and a most common material for solar cells has been the subject of a great deal of investigation both fundamental and technological over the past two decades. Although the semiconductors having energy gaps between 1.1 eV and 2.6 eV (InP, GaAs, AlSb, ZnSe, etc.) are most suitable for the fabrication of solar cells and the values of efficiency are higher than that of silicon. However, the absorption of ultraviolet radiation in the solar spectrum by the atmosphere and the occurrence of an intensity peak at about 5000 Å favours the semiconductor with smaller band gaps.

Although silicon is the most widely used semiconductor material, there are many other materials that are suitable for the fabrication of solar devices with acceptable characteristics. Some of these materials were studied as early as silicon (Milnes, 1972). Noh and Lec (1988) successfully fabricated SnO_2/*n*-Si solar cells using chemical vapour deposition (CVD) with conversion efficiency reaching 6.07%.

Franz *et al.* (1977) reported that SnO_2/Si junctions are inefficient for *p*-Si substrates but give good efficiency for *n*-Si substrates. Although SnO_2/*n*-Si solar cells are efficient, their stability is more strongly affected by the processing conditions.

An attempt has been made to emphasize the basic techniques involved in the fabrication of the SnO_2/*n*-Si solar cell and the study of variation of output power with various wavelengths of incident light in order to obtain maximum efficiency. The transmittance and absorption coefficient at different wavelengths for thin SnO_2 film have also been determined.

2. THEORY

Analysis (Anderson and Kent, 1975; Anderson, 1975) of the electrical properties indicates that SnO_2/Si solar cells are Schottky barrier with the expected barrier heights of 0.8 V for *n*-Si and 0.27–0.37 V for *p*-Si.

SnO_2 which has a high optical transparency and resistivity of the order of 2×10^{-3} Ω cm to 10^{-2} forms a heterojunction with silicon. It also serves at the same time as an antireflecting coating.

The basic theory of heterojunction solar cells has been briefly reviewed by Overstraeten and Mertens (1988).

3. FABRICATION OF Al–SnO_2–*n*Si SOLAR CELL

The wafers used in the fabrication of the cells were commercially available *n*-type polished Si wafers (FZ) of resistivity 6.5 Ω cm and ⟨100⟩ orientation.

In this section we briefly describe processes of wafer cleaning, formation of SnO_2 on silicon wafer as well as on a glass slide from chemical vapour deposition and metallization.

3.1. *Wafer cleaning*

(a) Wafers were boiled in trichloroethylene for 10 min to remove impurities like wax, resins and oil (molecular contaminants).
(b) Wafers were rinsed in distilled water for 5 min to wash away trichloroethylene.
(c) Heated in concentrated HNO_3 for 10 min to dissolve metallic impurities like Au, Ag, Cu, etc.
(d) Dipped in HF to remove oxides of impurities.
(e) Wafers were rinsed in hot distilled water for 10 min to remove traces of HNO_3 and HF.
(f) Finally wafers and the glass slide were put in an ultrasonic cleaner for 5 min to remove traces of dust particles.

After ultrasonic agitation, the cleaned wafers and the glass slide were taken directly to the next processing step.

3.2. *Formation of SnO_2 on Si*

An automizer-like arrangement as shown in Fig. 1 was used. The flask was filled with $SnCl_4$ which was heated by a gas burner to vaporize it. The Si wafer was kept under nozzle N at about 500°C. The air pushing bulb was worked to push ahead the mixture of air and $SnCl_4$ vapour.

$$SnCl_4 \xrightarrow{\text{Heat}} SnCl_2$$

$$O_2 + SnCl_2 \longrightarrow SnO_2 + Cl_2$$

$SnCl_2$ combined with oxygen of air forming SnO_2 on Si wafer.

3.3. *Formation of SnO_2 on a glass slide*

SnO_2 was also deposited on a glass slide which was kept at 400°C for the measurement of optical transmission spectra and the energy band gap of SnO_2 (see the Appendix).

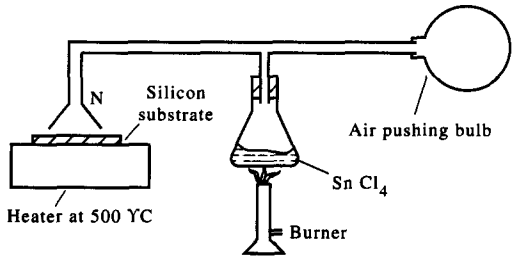

Fig. 1. Atomizer-like arrangement for the formation of SnO_2 layer on Si chips and glass slides.

3.4. *Metallization*

Pure Al (99.99%) was used for the contact as well as for front collecting grids and evaporation was done in vacuum coating under vacuum of the order of 10^{-5} Torr.

3.5. *Measurement of cell characteristics*

The load voltage measurements were made by varying the load using a rheostat of range 0–1750 Ω in conjunction with a resistance box of range 0–9000 Ω. The saturation current (I_{sc}) and open circuit voltage (V_{oc}) were measured without load. Experimental set-up is shown in Fig. 2. The Silicon Pyranometer with Integrator, Solar 118, was used to measure solar radiation intensity.

4. RESULTS

The illuminated current–voltage data for SnO_2/n-Si Schottky junction solar cell in different conditions are shown in Figs 3 and 4. These figures contains the results on the measurement of load current density J_L with load voltage V_L as the load R_L increases for solar radiation intensity $P_s = 95$, 75, 70 and 65 mW cm^{-2}.

Variation of open circuit voltage V_{oc} and short circuit current I_{sc} using blue, green and red filters are given in Table 1. Table 2 presents the variation of open circuit voltage V_{oc} and saturation current density J_s with solar intensity P_s.

Figures 5 and 6 present the open circuit

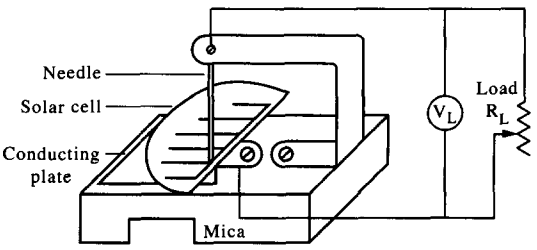

Fig. 2. Schematic diagram for the combined measuring set-up.

Table 1. Variation of open circuit voltage V_{oc} and short circuit current I_{sc} using different filters (solar intensity $P_s = 75$ mW cm^{-2})

Number	Filter	λ/nm	V_{oc}/mV	I_{sc}/μA	$V_{oc}/10^{-4}$ V^2
0	—	–	325	153.7	10.6
1	green	545	280	120.0	7.8
2	red$_1$	680	305	135.2	9.3
3	red$_2$	650	317	146.3	10.0
4	blue	450	298	131.2	8.9

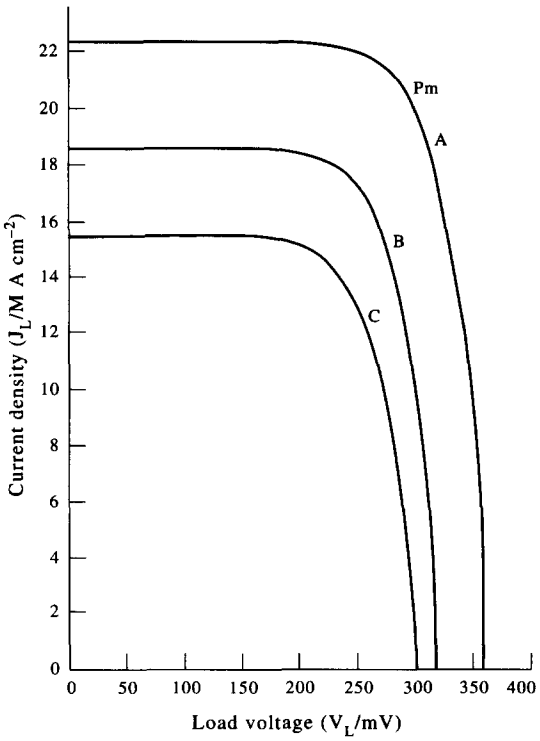

Fig. 3. Effect of light intensity on the load current density versus load voltage characteristics. Curve A: P_s = 95 mW cm^{-2}, V_{oc} = 360 mV, I_{sc} = 190 μA, I_0 = 0·17 nA. Curve B: P_s = 75 mW cm^{-2}, V_{oc} = 320 mV, I_{sc} = 175 μA, I_0 = 0.675 nA. Curve C, blue filter: P_s = 70 mW cm^{-2}, V_{ocb} = 301 mV, I_{scb} = 132 μA, I_{0b} = 1.16 nA.

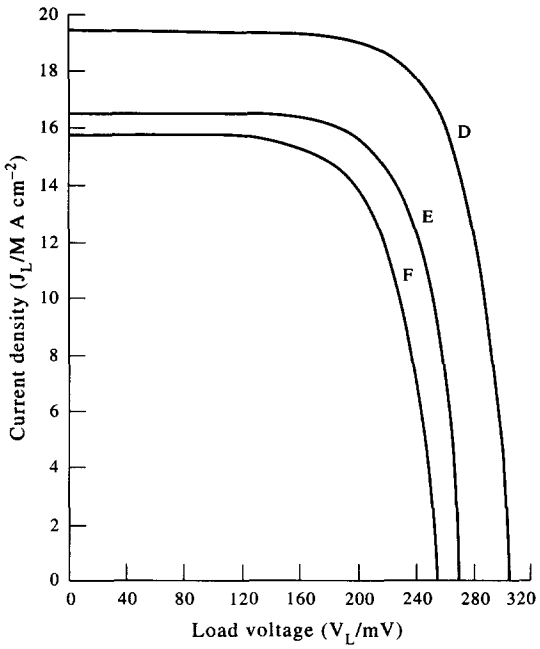

Fig. 4. Effect of light intensity on the load current density versus load voltage characteristics. Curve D, green filter: P_s = 70 mW cm^{-2}, V_{ocg} = 256 mV, I_{scg} = 136 μA, I_0 = 6·7 nA. Curve E, red filter: P_s = 70 mW cm^{-2}, V_{ocr} = 276 mV, I_{scr} = 141 μA, I_0 = 3.3 nA. Curve F, without filter: P_s = 65 mW cm^{-2}, V_{oc} = 306 mV, I_{sc} = 165 μA, I_0 = 1.2 nA.

voltage V_{oc}, short circuit current J_{sc} and power output $V_{oc}J_{sc}$ versus radiation intensity P_s.

Figure 7 shows the variation of I_0 with the solar radiation intensity P_s.

5. DISCUSSION

The load current density (J_L) versus load voltage (V_L) characteristics of the SnO_2/n-Si solar cell at a temperature of 27°C are presented in Figs 4 and 5. These figures compare the behaviour of the cell under different conditions of radiation intensities. Both direct and filtered sunlight follow the ideal characteristic curve, that is for a light beam of different colours, the short circuit current density J_{sc} is directly proportional to the intensity of light. Under illumination with sunlight of 95 mW cm^{-2} intensity, the cell gives an open circuit voltage (V_{oc}) of the order of 0.36, maximum power (P_{max}) of 6 mW cm^{-2}, maximum conversion efficiency (η_{max}) of 6.3% and fill factor (ff) of 0.75.

To provide further information about the conversion efficiency, the saturation current density J_s and open circuit voltage V_{oc} versus

Table 2. Variation of open circuit voltage V_{oc} and saturation current density J_s with solar radiation intensity P_s

P_s/ mW cm^{-2}	V_{oc}/mV	I_{sc}/μA	J_s/ mA cm^{-2}	$V_{oc}J_s$/ mV cm^{-2}
1	130	40.5	4.75	0.62
10	270	137.1	16.09	4.34
13	281	144.3	16.94	4.76
20	294	151.7	17.81	5.24
33	290	156.0	18.31	5.34
45	298	158.0	18.54	5.52
57	299	159.0	18.66	5.58
60	300	166.0	19.48	5.84
70	304	170.7	20.04	6.09
75	314	175.5	20.60	6.47
95	360	190.0	22.30	8.03

change in radiation intensity P_s measurements were made and compared as shown in Figs 3 and 4. It was realised that the J_s versus P_s as shown in Fig. 5 did not follow linear proportionality as expected. The current output did not increase rapidly with the small change in the initial illumination, on reaching about 10 mW cm^{-2} solar intensity the short circuit current begins to show almost constant value while the P_s increases.

An SnO_2/n-Si solar cell which has a heterojunction of band gaps 1.1 and 3.5 eV can generate a large photocurrent for wavelengths up to 1.1 μm. If the photocurrent is calculated based

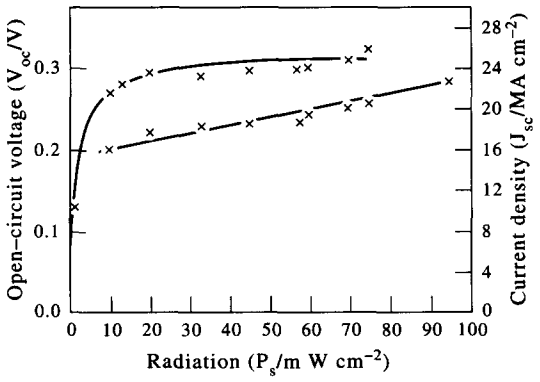

Fig. 5. Open-circuit voltage and short-circuit current as a function of light intensity.

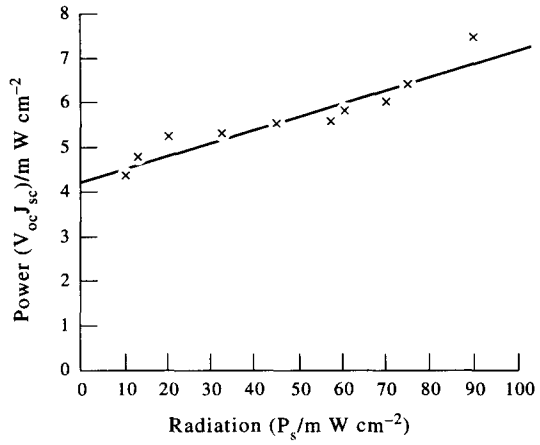

Fig. 6. Open-circuit power as a function of light intensity.

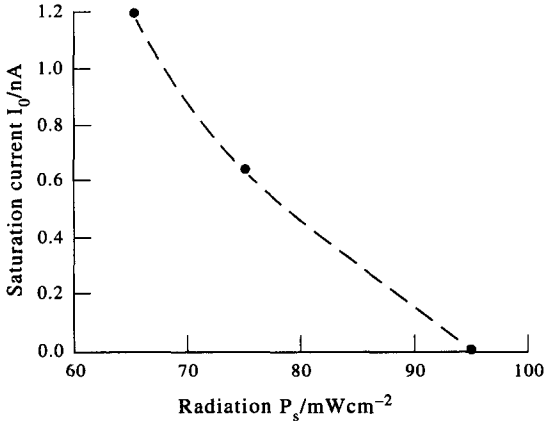

Fig. 7. Variation of I_0 with P_s.

on the 95 mW cm and assuming no recombination centres, the maximum photocurrent is about 35 mA cm^{-2}. A large portion of almost horizontal characteristic curve in Fig. 5 and the loss of photocurrent which may result from inhomogeneous deposition of SnO_2 on the Si wafer serving as recombination centres.

Much of the deviations in the curves were actually due to the inconsistency of the weather conditions during the period of measurement.

The maximum open circuit voltage and short circuit current density obtained were 0.36 V and 22.3 mA cm^{-2}, respectively, at 95 mW cm^{-2} solar intensity. This gives the conversion efficiency of 6.3% and comparably good fill factor of 0.75. Open circuit power and open circuit voltage as functions of light intensity are also presented in Tables 1 and 2 as well as in Figs 5 and 6, respectively.

From Fig. 7 it is evident that I_0 decreases as the solar radiation P_s increases. It is also observed that open circuit voltage V_{oc} and short circuit current I_{sc} increase as I_0 decreases.

In order for the efficiency of a solar cell to be high, both V_{oc} and J_{sc} have to be high. A large open circuit voltage V_{oc} requires a large short circuit current and a small dark saturation current. The reduction in I_0 at higher intensity is probably due to a decrease in stored minority carrier charge and also an increase in time constant, i.e. due to a decrease in lifetime and/or due to a decrease in the surface recombination velocity.

Further improvement in the efficiency may be obtained by changing the deposition condition of SnO_2 on Si. The stability and efficiency of SnO_2/*n*-Si solar cells may be related to the relatively small energy formation -124 kcal/mol for SnO_2 as compared to -192 kcal/mol for SiO_2.

It is quite obvious that under processing conditions reduction of SnO_2 is likely to occur by Si, i.e.:

$$SnO_2 + Si \rightleftharpoons SiO_2 + Sn$$

and there are indeed phenomena in the photocapacitance and in the *I–V* curves of SnO_2/Si solar cells that suggest a metal–insulator–semiconductor (MIS) structure (Anderson, 1975).

Improvements in the stability and efficiency can be obtained by changing the processing conditions.

NOMENCLATURE

P_s solar radiation intensity
V_{oc} open circuit voltage
I_{sc} short circuit current
I_0 saturation current
V_{ocb} open circuit voltage using blue filter
V_{ocg} open circuit voltage using green filter
V_{ocr} open circuit voltage using red filter

I_{scb} short circuit current using blue filter
I_{scg} short circuit current using green filter
I_{scr} short circuit current using red filter
I_{0b} saturation current using blue filter
I_{0g} saturation current using green filter
I_{0r} saturation current using red filter
max conversion efficiency
J_L load current density
V_L load voltage
R_L load
J_s saturation current density
J_{sc} short circuit current density

REFERENCES

Angrist S. W. (1972) *Direct Energy Conversion*, 3rd edn. Allyn and Bacon, Boston.
Anderson R. L. (1975) *Appl. Phys. Lett.* **27**, 691.
Anderson R. L. and Kent K. (1975) Final Report NSF/RANN/SE/AER74-AER74-17631/FR/75/3, Syracuse, New York, NTISPB-252949.
Arai T. J. (1964) *Phys. Soc. Jap.* **15**, 632.
Bennet H. E., Bennet J. M., Crowell C. R., Hirth J. P., Kerr D. R. and Chalmers B. (1976) *Sci. Am.* **14**, 174.
Franz S., Kent G. and Anderson R. L. (1977) *J. Electron. Mater.* **6**, 107.
Holland L. (1958) *Vacuum Deposition of Thin Films*, 1st edn. Wiley, New York.
Islam M. N. and Hakim M. O. (1985) *J. Mater. Sci. Lett.* **4**, 1129.
Kohnke E. E. and Hurt J. E. (1959) *Bull. Am. Phys. Soc.* **4**, 428.
Lawlen K. R., Mathews J. W., Moazed K. L., Perri J. A., Pliskin W. A. and Sze S. M. (1967) *Phys. Thin Films* **4**, 24.
Lim B. P. (1983) *Solar Energy Application in Tropics*, p. 165.
Loferski J. J. (1976) *Proc. 12th Photovoltaic Specialists Conf.*, IEEE, New York, p. 57.
Moss T. S. (1959) *Optical Properties of Semiconductors*, 1st edn. Butterworth, London.

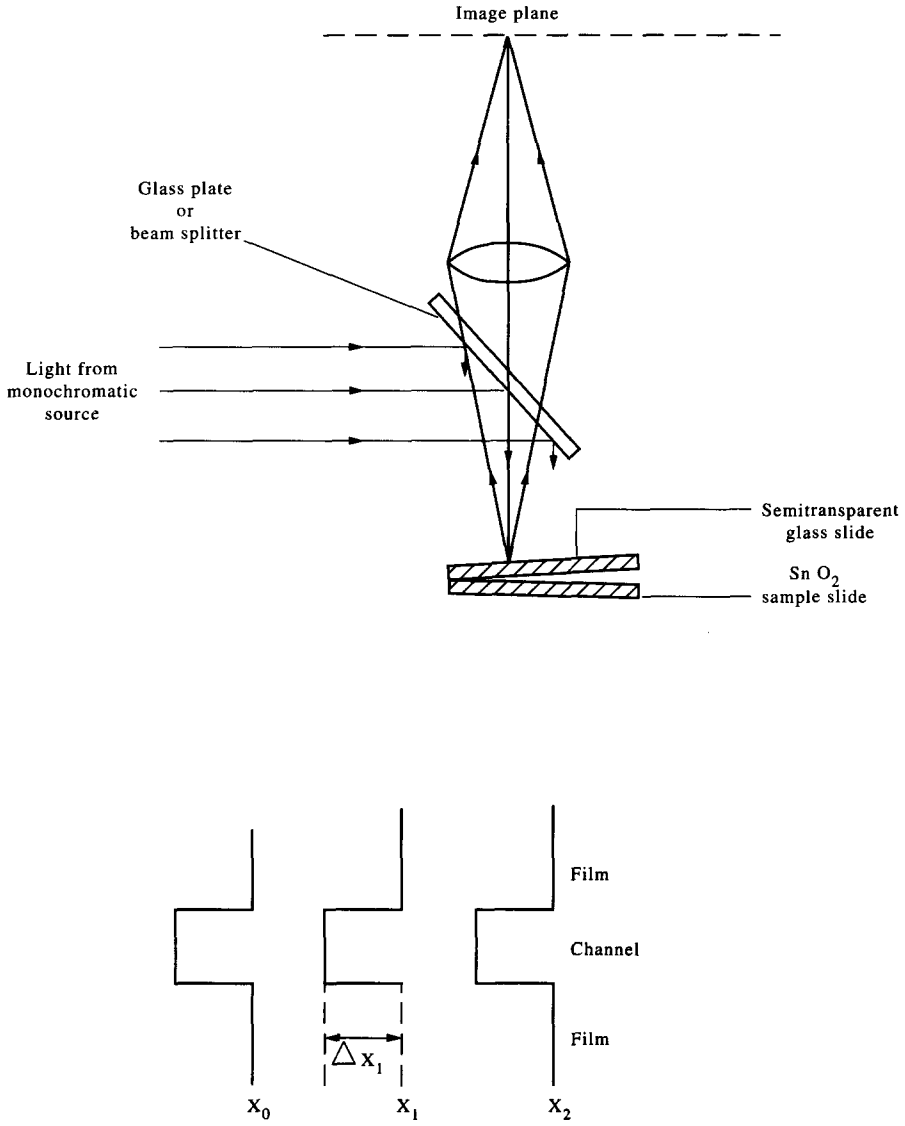

Fig. A1. Experimental arrangements for the measurement of film-thickness.

Manifacier J. C., Fillard J. P. and Bind J. M. (1981) *Thin Solid Films* **77**, 67.
Milnes A. G. and Feucht D. L. (1972) *Heterojunctions and Metal-Semiconductor Junctions*. Academy, New York.
Noh K. S., Sohn Y. K. and Lee D. H. (1988) *J. Solar Energy Soc. Korea* **8**, 19.
Neville R. C. (1978) *Solar Energy Conversion*. Elsevier, Amsterdam.
Overstraeten R. J. V. and Mertens R. P. (1986) *Physics, Technology and Use of Photovoltaics*. Adam Hilger, New York.
Sze S. M. (1981) *Physics of Semiconductor Devices*, 2nd edn. Wiley, New York.

APPENDIX

Determination of Transmission "T", Absorption Coefficient "α" and Energy Band Gap of SnO_2

An M_{40} Zeiss Specord UV-Visible spectrophotometer was used for the measurement of transmittance "T" and absorption coefficient "α" of the thin SnO_2 film deposited on the glass slide. The energy band gap of thin SnO_2 was also determined by plotting a graph of the variation of $(\alpha h\nu)^2$ with $h\nu$ and extrapolating the straight portion of the curve to $\alpha = 0$.

The internal transmission "T" of a material is related to the absorption coefficient (Manifacier *et al.*, 1981) by:

$$T = \exp(-\alpha t) \tag{A1}$$

where "t" is the thickness of the material.

Assuming that the transition probabilities become constant near the absorption edge, the absorption coefficient "α" for a direct allowed transition can be described as a function of the incident photon energy $h\nu$ (Moss, 1959).

$$\alpha = (h\nu - E_g)^{1/2}/h\nu \tag{A2}$$

where E_g is the energy band gap of the material.

From a plot of $(\alpha h\nu)^2$ against $h\nu$ the energy band gap E_g of SnO_2 can be determined by extrapolating the straight portion of the curve to $\alpha = 0$.

The thickness of the film was determined by interferometric method (Holland, 1958; Bernett *et al.*, 1967). The arrangement used consisted of two optically flat glass slides with one of them supporting the film sample is shown in Fig. A1 (top). The second glass slide was slanted and positioned directly above the film surface and it was illuminated with parallel monochromatic yellow light of wavelength 589 nm at normal incidence and viewed with a microscope. Dark and bright wedges were observed [Fig. A1 (bottom)]. The thickness of the film was calculated using

$$t = (\Delta x_1/x_1 - x_0) \cdot \lambda/2 \tag{A3}$$

where "λ" is the wavelength of the light used.

The thickness "t" of the SnO_2 film was determined to be 0.1. By substituting the value of "t" and the different values of transmission "T" obtained by the spectrophotometer for different values of wavelength "λ", the different values of the absorption coefficient "α" was obtained for the corresponding wavelengths.

From the graph of $(\alpha h\nu)^2$ versus $h\nu$ (Fig. A2) the energy band gap of SnO_2 was determined to be 3.43 eV, which was in good agreement with experimental values of 3.4 eV obtained by Arai (1964), 3.44 eV by Kohnke and Hurt (1959) and 3.45 eV by Islam and Hakim (1985).

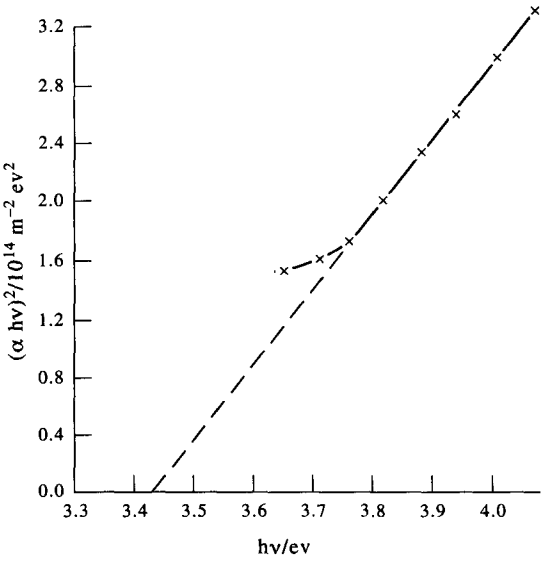

Fig. A2. Variation of $(\alpha h\nu)^2$ with $h\nu$.